Acta Cryst E
CRYSTALLOGRAPHIC COMMUNICATIONS

ISSN 2056-9890

Different classical hydrogen-bonding patterns in three salicylaldoxime derivatives, 2-HO-4-$XC_6H_3C{=}NOH$ (X = Me, OH and MeO)

Ligia R. Gomes,[a,b] **Marcus V. N. de Souza,**[c] **Cristiane F. Da Costa,**[c] **James Wardell**[c,d] **and John Nicolson Low**[d]*

[a]REQUIMTE, Departamento de Química e Bioquímica, Faculdade de Ciências da Universidade do Porto, Rua do Campo Alegre, 687, P-4169-007, Porto, Portugal, [b]FP-ENAS-Faculdade de Ciências de Saúde, Escola Superior de Saúde da UFP, Universidade Fernando Pessoa, Rua Carlos da Maia, 296, P-4200-150 Porto, Portugal, [c]Instituto de Tecnologia em Fámacos e Farmanguinhos, Fundação Oswaldo Cruz, 21041-250 Rio de Janeiro, RJ, Brazil, and [d]Department of Chemistry, University of Aberdeen, Meston Walk, Old Aberdeen, AB24 3UE, ., Scotland. *Correspondence e-mail: jnlow111@gmail.com

Received 18 September 2018
Accepted 19 September 2018

Edited by P. McArdle, National University of Ireland, Ireland

Keywords: crystal structure; hydrogen bonding; salicylaldoxime; Hirshfeld surface analysis.

CCDC references: 1868656; 1868655; 1868654

Supporting information: this article has supporting information at journals.iucr.org/e

The crystal structures of three salicyaldoxime compounds, namely 2-hydroxy-4-methylbenzaldehyde oxime, $C_8H_9NO_2$, **1**, 2,4-dihydroxybenzaldehyde oxime, $C_7H_7NO_3$, **2**, and 2-hydroxy-4-methoxybenzaldehyde oxime, $C_8H_9NO_3$, **3**, are discussed. In each compound, the hydroxyl groups are essentially coplanar with their attached phenyl group. The interplanar angles between the $C{=}N{-}O$ moieties of the oxime unit and their attached phenyl rings are 0.08 (9), 1.08 (15) and 6.65 (15)° in **1**, **2** and **3**, respectively. In all three molecules, the 2-hydroxy group forms an intramolecular $O{-}H\cdots N$(oxime) hydrogen bond. In compound (**1**), intermolecular $O{-}H$(oxime)$\cdots O$(hydroxyl) hydrogen bonds generate $R_2^2(14)$ dimers, related by inversion centres. In compound **2**, intermolecular $O{-}H$(oxime)$\cdots O$(4-hydroxy) hydrogen bonds generate $C9$ chains along the b-axis direction, while $O{-}H$(4-hydroxyl)$\cdots O$(2-hydroxyl) interactions form zigzag $C6$ spiral chains along the c-axis direction, generated by a screw axis at 1, y, 1/4: the combination of the two chains provides a bimolecular sheet running parallel to the b axis, which lies between 0–1/2 c and 1/2–1 c. In compound **3**, similar $C9$ chains, along the b-axis direction are generated by $O{-}H$(oxime)$\cdots O$(4-methoxy) hydrogen bonds. Further weaker, $C{-}H\cdots\pi$ (in **1**), π–π (in **2**) and both $C{-}H\cdots\pi$ and π–π interactions (in **3**) further cement the three-dimensional structures. Hirshfeld surface and fingerprint analyses are discussed.

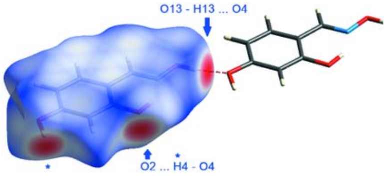

1. Chemical context

Aldoximes, $RCH{=}NOH$, are found in many biologically active compounds (Abele *et al.*, 2008; Nikitjuka & Jirgensons 2014), having a diverse range of uses including as anti-tumor agents (Martínez-Pascual *et al.*, 2017; Qin *et al.*, 2017; Canario *et al.*, 2018; Huang *et al.*, 2018), acaricidal and insecticidal agents (Dai *et al.*, 2017), thymidine phosphorylase inhibitors (Zhao *et al.*, 2018), anti-microbial agents (Yadav *et al.*, 2017), bacteriocides (Kozlowska *et al.*, 2017), anti-inflammatory agents (Mohassab *et al.*, 2017) and in the treatment of nerve-gas poisoning (Lorke *et al.*, 2008; Voicu *et al.*, 2010; Katalinić *et al.*, 2017; Radić *et al.*, 2013). In the plant kingdom, oximes play a vital role in metabolism (Sørensen *et al.*, 2018). A specific interest in 2-hydroxbenzaldehyde derivatives has arisen regarding their use as ligands for metal complexation (Wood *et al.*, 2006, 2008*b*).

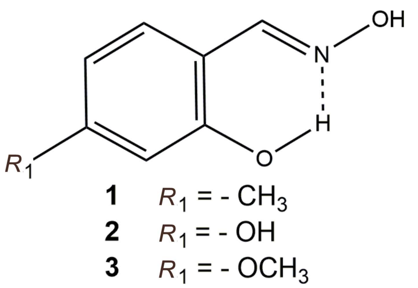

The compounds described herein are all salicylaldoxime derivatives (2-HO-4-*X*-C_6H_3-CH═NOH) with different substituents in the 4-position, namely a methyl group, a hydroxy group and a methoxy group, respectively, in compounds, **1**, **2** and **3**. A frequent finding for salicylaldoxime derivatives is the formation of inversion-related $R_2^2(14)$ dimers, as concluded from a Cambridge Structural Database survey (CSD Version 5.39, May 2018 update; Groom *et al.*, 2016). While the structures of many salicylaldoxime derivatives have been reported, the structures of very few compounds with an additional substituent in the 4 position are known.

Compounds **1** and **3** have been shown to have significant activity against *Mycobacterium tuberculosis* ATTC 27294. The full report will be published elsewhere (da Costa *et al.*, 2018).

2. Structural commentary

There are no unusual features in the molecular structures. Compound **1** (Fig. 1) crystallizes in the monoclinic space group $P2_1/n$ with one molecule in the asymmetric unit. Compounds **2** and **3** crystallize in the monoclinic space group $P2_1/c$ with one molecule in the asymmetric unit (Figs. 2 and 3), all having an oxime unit with an (*E*) geometry. Bond angles and bond lengths in the phenyl and oxime fragments are all in the expected ranges.

Table 1
Hydrogen-bond geometry (Å, °) for **1**.

Cg is the centroid of the C1–C6 ring.

$D—H\cdots A$	$D—H$	$H\cdots A$	$D\cdots A$	$D—H\cdots A$
$O2—H2\cdots N12$	0.879 (18)	1.814 (18)	2.6066 (10)	149.0 (15)
$O13—H13\cdots O2^{i}$	0.857 (17)	2.019 (17)	2.8132 (9)	153.7 (15)
$O13—H13\cdots O13^{ii}$	0.857 (17)	2.611 (16)	2.8961 (14)	100.8 (12)
$C3—H3\cdots Cg^{iii}$	0.95	2.71	3.4577 (9)	136
$C11—H11\cdots Cg^{iv}$	0.95	2.73	3.4910 (9)	138

Symmetry codes: (i) $-x+1, -y+1, -z+1$; (ii) $-x, -y+1, -z+1$; (iii) $-x+\frac{3}{2}, y+\frac{1}{2}, -z+\frac{1}{2}$; (iv) $-x+\frac{1}{2}, y-\frac{1}{2}, -z+\frac{1}{2}$.

In compound **1**, the hydroxyl group is essentially coplanar with its attached phenyl group [displaced by 0.020 (1) Å], while the interplanar angle between the C═NO moiety of the oxime unit and the attached phenyl rings is 0.08 (9)°. In compound **2**, the hydroxyl groups lie essentially within the phenyl ring plane [O atoms deviate by −0.003 (1) and 0.006 (1) Å], while the interplanar angle between the C═NO moiety of the oxime unit and the attached phenyl rings is 1.08 (15)°. In compound **3**, the interplanar angle between the C═NO moiety of the oxime unit and the attached phenyl rings is 6.65 (15)°.

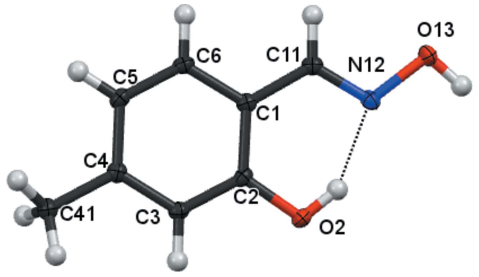

Figure 1
The molecular structure of compound **1**, showing 80% displacement ellipsoids.

In all three molecules, an intramolecular O2—H2···N12 hydrogen bond (Tables 1–3) forms a pseudo six-membered ring.

3. Supramolecular features

3.1. Hydrogen Bonding

In the crystal of **1**, molecules are linked by O13—H13 ···O2 hydrogen bonds into inversion-related $R_4^4(14)$ dimers (Table 1). As stated above, such dimers are the most frequently found arrangement for salicyldoxime derivatives. These $R_2^2(14)$, or $R_4^4(10)$ (*via* the intramolecular hydrogen bond) dimers are linked into two-molecule-wide chains, propagating in the *a*-axis direction by pairs of O13—

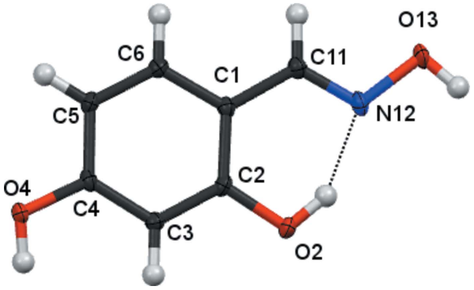

Figure 2
The molecular structure of compound **2**, showing 80% displacement ellipsoids.

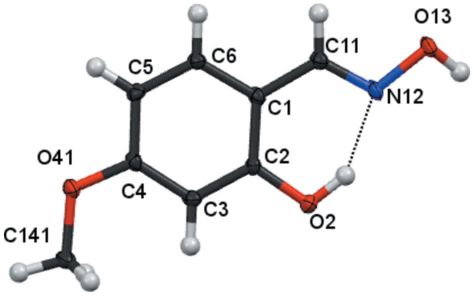

Figure 3
The molecular structure of compound **3**, showing 80% displacement ellipsoids.

Table 2
Hydrogen-bond geometry (Å, °) for **2**.

D—H···*A*	*D*—H	H···*A*	*D*···*A*	*D*—H···*A*
O2—H2···N12	0.91 (3)	1.77 (3)	2.5899 (17)	150 (2)
O4—H4···O2^{i}	0.86 (2)	1.85 (2)	2.7062 (16)	174 (2)
O13—H13···O4^{ii}	0.86 (3)	1.90 (3)	2.7583 (16)	171 (2)

Symmetry codes: (i) $-x+2, y+\frac{1}{2}, -z+\frac{1}{2}$; (ii) $x-1, y-1, z$.

Table 3
Hydrogen-bond geometry (Å, °) for **3**.

Cg is the centroid of the C1–C6 ring.

D—H···*A*	*D*—H	H···*A*	*D*···*A*	*D*—H···*A*
O2—H2···N12	0.92 (3)	1.81 (3)	2.6518 (19)	152 (2)
O13—H13···O41^{i}	0.91 (3)	1.89 (3)	2.7829 (18)	169 (3)
C141—H14*B*···O2^{ii}	0.98	2.62	3.412 (2)	138
C3—H3···O2^{ii}	0.95	2.70	3.570 (2)	154
C11—H11···*Cg*^{iii}	0.95	2.89	3.4524 (6)	128

Symmetry codes: (i) $x+1, y, z$; (ii) $-x+1, -y, -z+1$; (iii) $-x+1, y+\frac{1}{2}, -z+\frac{1}{2}$.

H13···O13 hydrogen bonds, thereby creating $R_2^2(4)$ rings, as shown in Fig. 4. The H13···O13 lengths in the O13—H13···O13^{ii} hydrogen bond are rather long [2.611 (16) Å] with a small angle of 100.8 (12)°. However, such data fits well with published findings for H_2O_2 rings: a recent CSD (Groom *et al.*, 2016) search revealed more than 500 entries for non-solvated structures having centrosymmetric H_2O_2 rings with H—O—H angles of 120° or less and H···O distances up to the sum of the van der Waals contact radii, 2.72 Å, of oxygen and hydrogen atoms. The two-molecule-wide chains are further linked into a three-dimensional arrangement by C3—H3···*Cg*^{iii} and C11—H11··· *Cg*^{iv} interactions (Table 1). No π–π interactions can be identified.

Compound **2** with two hydroxyl groups, as well as the oxime moiety, produces a much more complex classical hydrogen-bonding arrangement than the one found for compound **1**. The bonding arrangement in **2** can be readily considered to be composed of two elements: a *C*9 chain, generated from O13—H13(oxime)···O4(4-hydroxy)^{ii} hydrogen bonds, propagating in the direction of the *b* axis, see Fig. 5, and secondly a zigzag *C*6 spiral chain formed from O4—H4···O2^{i} hydrogen bonds, see Fig. 6. The C6 and C9 chains combine to form a bimolecular sheet running parallel to the *b* axis which lies between 0–$\frac{1}{2}$ *c* and $\frac{1}{2}$–1 *c*. These sheets are further linked by moderately strong π–π stacking interactions, involving all the phenyl rings in the sheet: the *Cg*···*Cg* separation is 3.7242 (13) Å with a phenyl ring slippage of 1.586 Å. The lack of an $R_2^2(14)$ dimer in **2** is apparent and results from the preferential interaction of the oxime group with the 4-hydroxyl group rather than with the 2-hydroxy group.

In compound **3**, *C*9 chains are generated from O13—H13···O41(methoxy)^{i} hydrogen bonds, which propagate in the direction of the *b* axis, see Fig. 7. This chain is similar to that found in compound **2**, but involving the methoxy oxygen

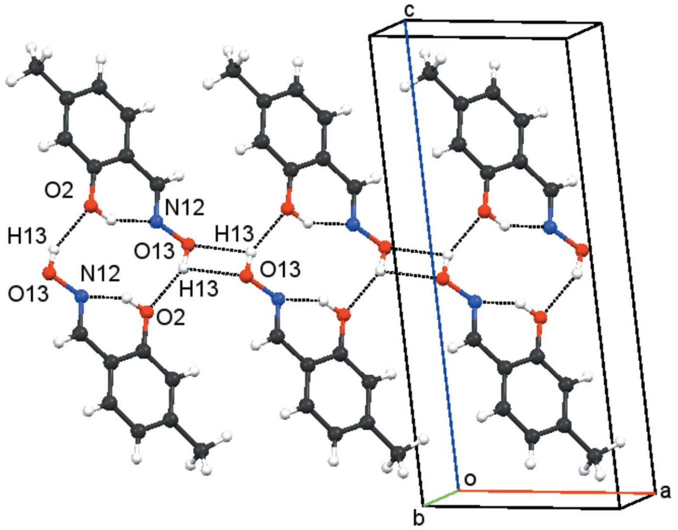

Figure 4
Part of a two-molecule-wide chain in **1** (symmetry codes as in Table 1).

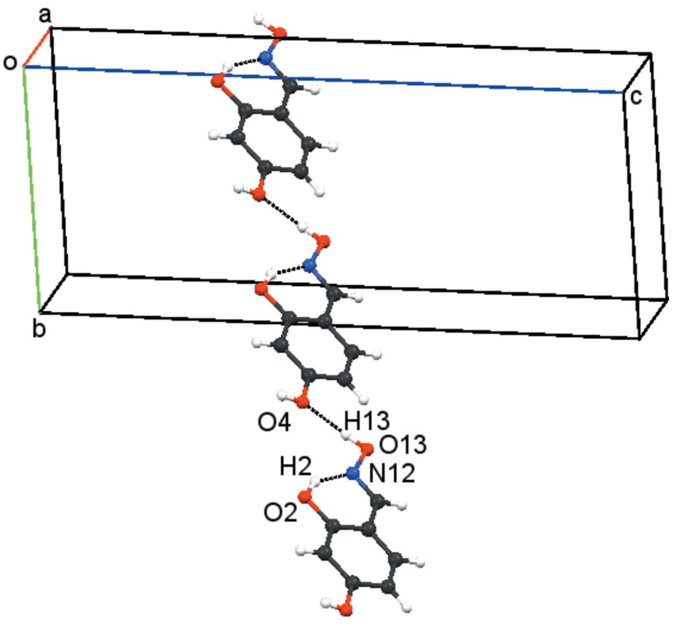

Figure 5
Compound **2**. Part of a *C*9 chain, propagating in the *b*-axis direction, formed by O13—H13···O4 hydrogen bonds.

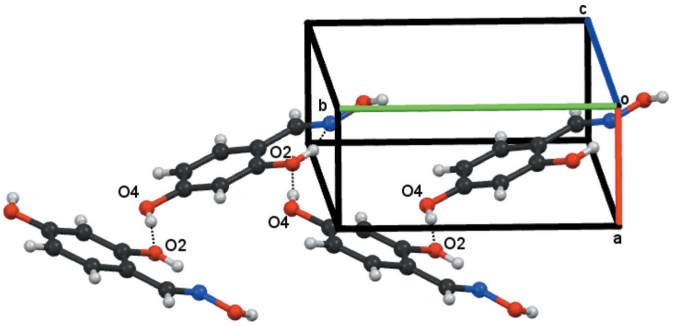

Figure 6
Compound **2**, part of a spiral *C*6 chain formed from O4—H4···O2 hydrogen bonds

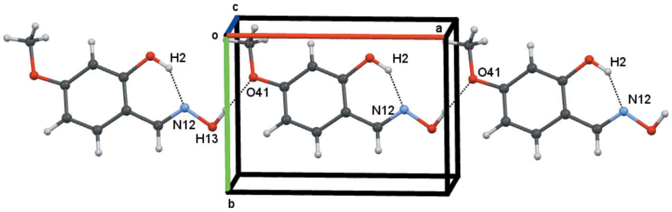

Figure 7
Compound **3**, part of a *C*9 chain of molecules formed by O13—H13···O41 hydrogen bonds, propagating along the *a*-axis direction.

atom O41 involved instead of the hydroxy oxygen O4. Interestingly, the parameters of the two hydrogen bonds in the chains of compound **2** and **3** are very similar. The chains in compound **3** are linked into a two-dimensional array by C11—H11···*Cg* (Table 3) and π–π interactions. The centroid–centroid separation in the π–π interaction is 3.7926 (12) Å with a phenyl ring slippage of 1.571 Å – again similar parameters are found in the interactions of compounds **2** and **3**. The lack of an $R_2^2(14)$ dimer results from the preferential interaction of the oxime group with the 4-methoxy group rather than with the 2-hydroxy group. The C141—H14*B*···O2$^{\rm ii}$ and C3—H3···O2$^{\rm iii}$ hydrogen bonds link the molecules into centrosymmetric dimers across the centre of symmetry at ($\frac{1}{2}$, 0, $\frac{1}{2}$). The former hydrogen bond forms $R_2^2(14)$ rings, and the latter $R_2^2(8)$ rings. These link anti-parallel *C*9 chains, forming a corrugated ribbon which runs parallel to the *a* axis.

Table 4
Percentages of atom–atom contacts for compounds **1**–**3**.

Compound	1	2	3
H···H	42.7	36.9	41.5
H···O/O···H	21.4	33.8	27.9
H···C/C···H	29.1	10.0	15.5
H···N/N···H	5.4	2.9	4.1
C···C	–	10.8	5.8
O···C/C···O	1.2	2.2	3.1
N···O/O···N	–	2.0	0.7
N···C/C···N	–	–	–
O···O	0.2	–	–

3.2. Hirshfeld Surface Analyses

The Hirshfeld surfaces (Spackman & Jayatilaka, 2009) and two-dimensional fingerprint (FP) plots (Spackman & McKinnon, 2002) provide complementary information concerning the intermolecular interactions discussed above. The analyses were generated using *CrystalExplorer3.1* (Wolff *et al.*, 2012). The Hirshfeld surfaces mapped over $d_{\rm norm}$ for **1**–**3** are illustrated in Fig. 8. The intense red areas on the surfaces correspond to O···H close contacts. The less intense red spot on the surface of **1** relates to a O···O short contact. The fingerprint plots are shown in Fig. 9. The percentage contributions to the Hirshfeld surface of the various atom···atom contacts shown in Table 4 are derived from the fingerprint plots.

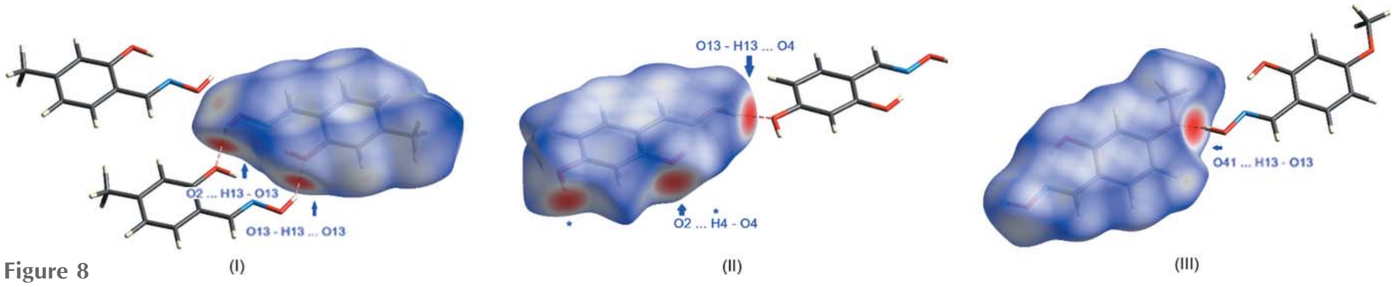

Figure 8
Views of the Hirshfeld surfaces mapped over $d_{\rm norm}$ for **1**–**3**. In each case, the red areas relate to classical hydrogen bonds.

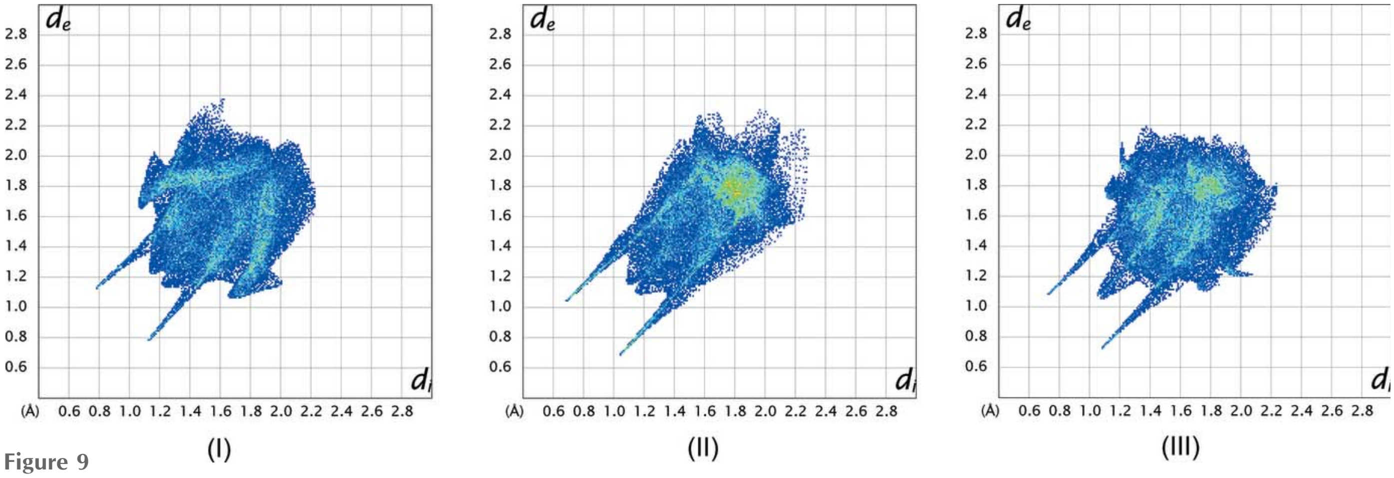

Figure 9
The FP plots for **1**, **2** and **3**. The pair of southwest spikes are due to the O···H /H···O close contacts. The highest intensity of pixels in the FP plot for **2** at d_e/d_i = 1.8 Å includes C···C contacts.

Table 5
Experimental details.

	1	**2**	**3**
Crystal data			
Chemical formula	$C_8H_9NO_2$	$C_7H_7NO_3$	$C_8H_9NO_3$
M_r	151.16	153.14	167.16
Crystal system, space group	Monoclinic, $P2_1/n$	Monoclinic, $P2_1/c$	Monoclinic, $P2_1/c$
Temperature (K)	100	100	100
a, b, c (Å)	6.5507 (2), 7.2523 (2), 15.5478 (4)	3.7241 (1), 8.6902 (2), 20.7570 (5)	9.3591 (13), 6.2634 (7), 13.6260 (2)
β (°)	96.737 (3)	92.501 (2)	108.636 (16)
V (Å^3)	733.54 (4)	671.12 (3)	756.87 (15)
Z	4	4	4
Radiation type	Mo $K\alpha$	Mo $K\alpha$	Mo $K\alpha$
μ (mm^{-1})	0.10	0.12	0.11
Crystal size (mm)	0.25 × 0.15 × 0.02	0.20 × 0.10 × 0.05	0.15 × 0.05 × 0.01
Data collection			
Diffractometer	Rigaku FRE+ AFC12 with HyPix 6000 detector	Rigaku FRE+ AFC12 with HyPix 6000 detector	Rigaku FRE+ AFC12 with HyPix 6000 detector
Absorption correction	Multi-scan (*CrysAlis PRO* ; Rigaku OD, 2017)	Multi-scan (*CrysAlis PRO* ; Rigaku OD, 2017)	Multi-scan (*CrysAlis PRO*; Rigaku OD, 2017)
T_{min}, T_{max}	0.742, 1.000	0.654, 1.000	0.305, 1.000
No. of measured, independent and observed [$I > 2\sigma(I)$] reflections	16323, 1696, 1560	29482, 1537, 1482	5525, 1686, 1323
R_{int}	0.024	0.039	0.060
$(\sin \theta/\lambda)_{max}$ (Å^{-1})	0.649	0.649	0.648
Refinement			
$R[F^2 > 2\sigma(F^2)]$, $wR(F^2)$, S	0.032, 0.100, 1.08	0.040, 0.092, 0.86	0.049, 0.158, 1.01
No. of reflections	1696	1537	1686
No. of parameters	109	113	118
H-atom treatment	H atoms treated by a mixture of independent and constrained refinement	H atoms treated by a mixture of independent and constrained refinement	H atoms treated by a mixture of independent and constrained refinement
$\Delta\rho_{max}$, $\Delta\rho_{min}$ (e Å^{-3})	0.33, −0.20	0.38, −0.21	0.26, −0.29

Computer programs: *CrysAlis PRO* (Rigaku OD, 2017), *OSCAIL* (McArdle *et al.*, 2004), *SHELXT* (Sheldrick, 2015*a*), *ShelXle* (Hübschle *et al.*, 2011), *SHELXL2017/1* (Sheldrick, 2015*b*), *Mercury* (Macrae *et al.*, 2006) and *PLATON* (Spek, 2009).

There are some differences in the percentage of close contacts listed in Table 4 between the $R_2^2(14)$ dimer formed by compound **1** and the molecular chains formed by compounds **2** and **3**. Thus compound **1** exhibits the highest percentage of H···C/ C···H close contacts, but no C···C and N···O/ O···N close contacts, unlike compounds **2** and **3**, and is the only one of the three compounds to have any close O···O contacts, albeit a very small percentage. It has to be said that the different substituents, especially the number of hydroxyl units, and other interactions, such as C—H···π and π–π interactions, will have significant effects on the hydrogen-bonding.

4. Database survey

A survey of the Cambridge Structural Database (CSD Version 5.39, May 2018 update; Groom *et al.*, 2016) of the hydrogen-bonding patterns of oximes confirmed the invariable occurrence for salicylaldoximes, *R*—CH═N—OH (where *R* is a 2-hydroxyphenyl derivative) of the formation of intramolecular O—H···NO(oxime) hydrogen bonds involving the *ortho* hydroxyl group. In addition, this hydroxyl group is also most frequently involved in intermolecular interactions producing inversion-related $R_2^2(14)$ dimers (Smith *et al.*, 2003; Wood *et al.*, 2006, 2008*b*). Exceptions include MXSALO [*R* = 2-HO-5-MeOC$_6$H$_3$, producing a *C*5 chain from O—H(oxime)···O(2-hydroxyl) hydrogen bonds; Pfluger *et al.*, 1978], YUPSOT [*R* = 2-HO-5-^{t}Bu-C$_6$H$_3$, producing a *C*5 chain from O—H(oxime)···O(2-hydroxyl) hydrogen bonds; White *et al.*, 2015*a*], YUPROS [*R* = 2-HO-3-Me-5-(piperin-1-yl-CH$_2$)-C$_6$H$_2$, producing a *C*9 chain from O—H(oxime)···N(piperinyl) hydrogen bonds; White *et al.*, 2015*b*] and XUSPIL [*R* = 2-HO-3-(piperin-1-ylmethyl)-5-^{t}Bu-C$_6$H$_2$, producing a *C*9 chain from O—H(oxime)···N(piperinyl) hydrogen bonds; Forgan *et al.*, 2010].

The compounds 2-HO-3-MeOC$_6$H$_3$CH═N—OH (ABULIT01–07; Forgan *et al.*, 2007; Wood *et al.*, 2008*a*) and 2-HO-3-EtOC$_6$H$_3$CH═N—OH (HAHGAA; Cai, 2011) both form $R_2^2(14)$ dimers, in contrast to the chain forming 2-HO-4-MeOC$_6$H$_3$CH═N—OH (this study) and 2-HO-5-MeOC$_6$H$_3$CH═N—OH (MXSALO; Pfluger *et al.*, 1978) and 2-HO-5-^{t}BuOC$_6$H$_3$CH═N—OH (YUPSOT; White *et al.*, 2015*a*).

An earlier search (Low *et al.*, 2010) indicated that the most frequently found hydrogen-bonding arrangements for oximes without a 2-hydroxyphenyl group are inversion-related $R_2^2(6)$ dimers and *C*3 chains.

5. Synthesis and crystallization

The title compounds were prepared from hydroxylamine and the corresponding benzaldehyde in methanol in the presence of potassium carbonate and were recrystallized from methanol. Compound **1**, m.p. 378–379 K. Compound **2**, m.p. 451–452 K. Compound **3**, m.p. 410–411 K.

6. Refinement details

Crystal data, data collection and structure refinement details are summarized in Table 5. All hydroxyl H atoms were refined isotropically. Those attached to C atoms were refined as riding atoms with C—H = 0.95–0.98 Å and $U_{\rm iso}$(H) = 1.2–1.5$U_{\rm iso}$(C).

Acknowledgements

The authors thank the staff at the National Crystallographic Service, University of Southampton (Coles & Gale, 2012), for the data collection, help and advice.

References

Abele, E., Abele, R. & Lukevics, E. (2008). *Chem. Heterocycl. Cmpd*, **44**, 769–792.

Cai, L.-F. (2011). *Z. Kristallogr. New Cryst. Struct.* **226**, 315–316.

Canario, C., Silvestre, S., Falcao, A. & Alves, G. (2018). *Curr. Med. Chem.* **25**, 660–686.

Coles, S. J. & Gale, P. A. (2012). *Chem. Sci.* **3**, 683–689.

Costa, C. F. da, Lourenço, M. C. S., Coimbra, E. S., Carvalho, G. S., Wardell, J. L., Calixto, S. L., Granato, J. T. & de Souza, M. V. N. (2018). Unpublished observations.

Dai, H., Chen, J., Li, G., Ge, S. S., Shi, Y. J., Fang, Y. & Ling, Y. (2017). *Bioorg. Med. Chem. Lett.* **27**, 950–953.

Forgan, R. S., Davidson, J. E., Fabbiani, F. P. A., Galbraith, S. G., Henderson, D. K., Moggach, S. A., Parsons, S., Tasker, P. A. & White, F. J. (2010). *Dalton Trans.* **39**, 1763–1770.

Forgan, R. S., Wood, P. A., Campbell, J., Henderson, D. K., McAllister, F. E., Parsons, S., Pidcock, E., Swart, R. M. & Tasker, P. A. (2007). *Chem. Commun.* pp. 4940–4942.

Groom, C. R., Bruno, I. J., Lightfoot, M. P. & Ward, S. C. (2016). *Acta Cryst.* B**72**, 171–179.

Huang, G., Zhao, H. R., Meng, Q. Q., Zhang, Q. J., Dong, J. Y., Zhu, B. Q. & Li, S. S. (2018). *Eur. J. Med. Chem.* **143**, 166–181.

Hübschle, C. B., Sheldrick, G. M. & Dittrich, B. (2011). *J. Appl. Cryst.* **44**, 1281–1284.

Katalinić, M., Zandona, A., Ramić, A., Zorbaz, T., Primožič, I. & Kovarik, Z. (2017). *Molecules*, **22**, No. 1234.

Kozlowska, J., Potaniec, B., Zarowska, B. & Aniol, M. (2017). *Molecules*, **22** No. 1485.

Lorke, D. E., Kalasz, H., Petroianu, G. A. & Tekes, K. (2008). *Curr. Med. Chem.* **15**, 743–753.

Low, J. N., Santos, L. M. N. B. F., Lima, C. F. R. A. C., Brandão, P. & Gomes, L. R. (2010). *Eur. J. Chem.* **1**, 61–66.

Macrae, C. F., Edgington, P. R., McCabe, P., Pidcock, E., Shields, G. P., Taylor, R., Towler, M. & van de Streek, J. (2006). *J. Appl. Cryst.* **39**, 453–457.

Martínez-Pascual, R., Meza-Reyes, S., Vega-Baez, J. L., Merino-Montiel, P., Padrón, J. M., Mendoza, Á. & Montiel-Smith, S. (2017). *Steroids*, **122**, 24–33.

McArdle, P., Gilligan, K., Cunningham, D., Dark, R. & Mahon, M. (2004). *CrystEngComm*, **6**, 303–309.

Mohassab, M., Hassan, H. A., Abdelhamid, D., Abdel-Aziz, M., Dalby, K. N. & Kaoud, T. S. (2017). *Bioorg. Chem.* **75**, 242–259.

Nikitjuka, A. & Jirgensons, A. (2014). *Chem. Heterocycl. C.* **49**, 1544–1559.

Pfluger, C. E., Pfluger, M. T. & Brackett, E. B. (1978). *Acta Cryst.* B**34**, 1017–1019.

Qin, H. L., Leng, J., Youssif, B. G. M., Amjad, M. W., Raja, M. A. G., Hussain, M. A., Hussain, Z., Kazmi, S. N. & Bukhari, S. N. A. (2017). *Chem. Biol. Drug Des.* **90**, 443–449.

Radić, Z., Dale, T., Kovarik, Z., Berend, S., Garcia, E., Zhang, L., Amitai, G., Green, C., Radić, B., Duggan, B. M., Ajami, D., Rebek, J. Jr & Taylor, P. (2013). *Biochem. J.* **450**, 231–242.

Rigaku OD (2017). *CrysAlis* PRO. Rigaku Oxford Diffraction, Yarnton, England.

Sheldrick, G. M. (2015*a*). *Acta Cryst.* A**71**, 3–8.

Sheldrick, G. M. (2015*b*). *Acta Cryst.* C**71**, 3–8.

Smith, A. G., Tasker, P. & White, D. J. (2003). *Coord. Chem. Rev.* **241**, 61–85.

Sørensen, M., Neilson, E. H. J. & Møller, B. L. (2018). *Mol. Plant.* **11**, 95–117.

Spackman, M. A. & Jayatilaka, D. (2009). *CrystEngComm*, **11**, 19–32.

Spackman, M. A. & McKinnon, J. J. (2002). *CrystEngComm*, **4**, 378–392.

Spek, A. L. (2009). *Acta Cryst.* D**65**, 148–155.

Voicu, V. A., Thiermann, H., Rădulescu, F. Ş., Mircioiu, C. & Miron, D. S. (2010). *Basic Clin. Pharmacol. Toxicol.* **106**, 73–85.

White, F., Forgan, R. & Tasker, P. (2015*b*). Private communication (refcode 1410307). CCDC, Cambridge, England.

White, F., Gordon, R. & Tasker, P. (2015*a*). Private communication (refcode 1410312). CCDC, Cambridge, England.

Wolff, S. K., Grimwood, D. I., McKinnon, J. J., Turner, M. J., Jayatilaka, D. & Spackman, M. A. (2012). *Crystal Explorer*. The University of Western Australia.

Wood, P. A., Forgan, R. S., Henderson, D., Lennie, A. R., Parsons, S., Pidcock, E., Tasker, P. A. & Warren, J. E. (2008*a*). *CrystEngComm*, **10**, 259–251.

Wood, P. A., Forgan, R. S., Henderson, D., Parsons, S., Pidcock, E., Tasker, P. A. & Warren, J. E. (2006). *Acta Cryst.* B**62**, 1099–1111.

Wood, P. A., Forgan, R. S., Lennie, A. R., Parsons, S., Pidcock, E., Tasker, P. A. & Warren, J. E. (2008*b*). *CrystEngComm*, **10**, 239–251.

Yadav, P., Lal, K., Rani, P., Mor, S., Kumar, A. & Kumar, A. (2017). *Med. Chem. Res.* **26**, 1469–1480.

Zhao, S. Y., Li, K., Jin, Y. & Lin, J. (2018). *Eur. J. Med. Chem.* **144**, 41–51.

supporting information

Acta Cryst. (2018). E**74**, 1480-1485   [https://doi.org/10.1107/S2056989018013361]

Different classical hydrogen-bonding patterns in three salicylaldoxime derivatives, 2-HO-4-*X*C_6H_3C&z-dbnd;NOH (*X* = Me, OH and MeO)

Ligia R. Gomes, Marcus V. N. de Souza, Cristiane F. Da Costa, James Wardell and John Nicolson Low

Computing details

For all structures, data collection: *CrysAlis PRO* (Rigaku OD, 2017); cell refinement: *CrysAlis PRO* (Rigaku OD, 2017); data reduction: *CrysAlis PRO* (Rigaku OD, 2017); program(s) used to solve structure: *OSCAIL* (McArdle *et al.*, 2004), SHELXT (Sheldrick, 2015a). Program(s) used to refine structure: *OSCAIL* (McArdle *et al.*, 2004), *ShelXle* (Hübschle *et al.*, 2011), *SHELXL2017/1* (Sheldrick, 2015b) for (1), (2); *OSCAIL* (McArdle *et al.*, 2004), *ShelXle* (Hübschle *et al.*, 2011), *SHELXL2017*/1 (Sheldrick, 2015b) for (3). For all structures, molecular graphics: *Mercury* (Macrae *et al.*, 2006); software used to prepare material for publication: *OSCAIL* (McArdle *et al.*, 2004), *SHELXL2017/1* (Sheldrick, 2015b), *PLATON* (Spek, 2009).

2-Hydroxy-4-methylbenzaldehyde oxime (1)

Crystal data

$C_8H_9NO_2$	$F(000) = 320$
$M_r = 151.16$	$D_x = 1.369$ Mg m^{-3}
Monoclinic, $P2_1/n$	Mo $K\alpha$ radiation, $\lambda = 0.71075$ Å
$a = 6.5507$ (2) Å	Cell parameters from 8222 reflections
$b = 7.2523$ (2) Å	$\theta = 3.1$–$31.9°$
$c = 15.5478$ (4) Å	$\mu = 0.10$ mm^{-1}
$\beta = 96.737$ (3)°	$T = 100$ K
$V = 733.54$ (4) Å^3	Plate, brown
$Z = 4$	0.25 × 0.15 × 0.02 mm

Data collection

Rigaku FRE+ AFC12 with HyPix 6000 detector diffractometer	$T_{min} = 0.742$, $T_{max} = 1.000$
Radiation source: Rotating Anode, Rigaku FRE+	16323 measured reflections
Confocal mirrors, VHF Varimax monochromator	1696 independent reflections
Detector resolution: 10 pixels mm^{-1}	1560 reflections with $I > 2\sigma(I)$
profile data from ω–scans	$R_{int} = 0.024$
Absorption correction: multi-scan (CrysAlisPro ; Rigaku OD, 2017)	$\theta_{max} = 27.5°$, $\theta_{min} = 2.6°$
	$h = -8 \rightarrow 8$
	$k = -9 \rightarrow 9$
	$l = -20 \rightarrow 20$

Refinement

Refinement on F^2
Least-squares matrix: full
$R[F^2 > 2\sigma(F^2)] = 0.032$
$wR(F^2) = 0.100$
$S = 1.08$
1696 reflections
109 parameters
0 restraints
Hydrogen site location: mixed
H atoms treated by a mixture of independent and constrained refinement
$w = 1/[\sigma^2(F_o^2) + (0.0569P)^2 + 0.1857P]$ where $P = (F_o^2 + 2F_c^2)/3$
$(\Delta/\sigma)_{max} < 0.001$
$\Delta\rho_{max} = 0.33$ e Å^{-3}
$\Delta\rho_{min} = -0.20$ e Å^{-3}

Special details

Geometry. All esds (except the esd in the dihedral angle between two l.s. planes) are estimated using the full covariance matrix. The cell esds are taken into account individually in the estimation of esds in distances, angles and torsion angles; correlations between esds in cell parameters are only used when they are defined by crystal symmetry. An approximate (isotropic) treatment of cell esds is used for estimating esds involving l.s. planes.

Fractional atomic coordinates and isotropic or equivalent isotropic displacement parameters (Å^2)

	x	*y*	*z*	U_{iso}*/U_{eq}
O2	0.62147 (10)	0.55213 (9)	0.38936 (4)	0.01715 (19)
H2	0.520 (3)	0.516 (2)	0.4176 (11)	0.046 (4)*
O13	0.11027 (10)	0.35295 (10)	0.46255 (4)	0.01893 (19)
H13	0.155 (2)	0.389 (2)	0.5139 (11)	0.041 (4)*
N12	0.27030 (11)	0.40720 (11)	0.41612 (5)	0.01501 (19)
C1	0.38496 (13)	0.41353 (12)	0.27677 (5)	0.0129 (2)
C2	0.57244 (13)	0.50209 (12)	0.30486 (5)	0.0131 (2)
C3	0.71163 (13)	0.54354 (12)	0.24671 (6)	0.0139 (2)
H3	0.837332	0.603208	0.266799	0.017*
C4	0.66904 (13)	0.49864 (12)	0.15934 (6)	0.0137 (2)
C5	0.48296 (14)	0.41041 (12)	0.13081 (6)	0.0144 (2)
H5	0.451750	0.379046	0.071398	0.017*
C6	0.34460 (13)	0.36875 (12)	0.18861 (6)	0.0139 (2)
H6	0.219471	0.308503	0.168196	0.017*
C11	0.23470 (13)	0.36707 (12)	0.33550 (6)	0.0139 (2)
H11	0.110265	0.306989	0.313953	0.017*
C41	0.81701 (14)	0.54974 (13)	0.09625 (6)	0.0173 (2)
H41A	0.814596	0.454650	0.051360	0.026*
H41B	0.956069	0.559362	0.126945	0.026*
H41C	0.776779	0.668498	0.069346	0.026*

Atomic displacement parameters (Å^2)

	U^{11}	U^{22}	U^{33}	U^{12}	U^{13}	U^{23}
O2	0.0175 (3)	0.0221 (4)	0.0115 (3)	−0.0050 (3)	0.0003 (2)	−0.0029 (2)
O13	0.0156 (3)	0.0260 (4)	0.0162 (3)	−0.0046 (3)	0.0059 (3)	−0.0030 (3)
N12	0.0137 (4)	0.0158 (4)	0.0162 (4)	−0.0005 (3)	0.0048 (3)	0.0001 (3)
C1	0.0133 (4)	0.0110 (4)	0.0141 (4)	0.0013 (3)	0.0009 (3)	0.0004 (3)
C2	0.0159 (4)	0.0114 (4)	0.0115 (4)	0.0016 (3)	−0.0009 (3)	−0.0006 (3)
C3	0.0135 (4)	0.0124 (4)	0.0153 (4)	−0.0004 (3)	−0.0001 (3)	0.0000 (3)

C4	0.0152 (4)	0.0112 (4)	0.0147 (4)	0.0020 (3)	0.0016 (3)	0.0009 (3)
C5	0.0166 (4)	0.0137 (4)	0.0124 (4)	0.0015 (3)	−0.0009 (3)	−0.0008 (3)
C6	0.0133 (4)	0.0122 (4)	0.0153 (4)	0.0005 (3)	−0.0016 (3)	−0.0009 (3)
C11	0.0132 (4)	0.0118 (4)	0.0164 (4)	0.0007 (3)	0.0007 (3)	−0.0005 (3)
C41	0.0177 (4)	0.0192 (4)	0.0153 (4)	−0.0016 (3)	0.0029 (3)	0.0000 (3)

Geometric parameters (Å, º)

O2—C2	1.3645 (10)	C3—H3	0.9500
O2—H2	0.879 (18)	C4—C5	1.4018 (13)
O13—N12	1.3973 (9)	C4—C41	1.5041 (12)
O13—H13	0.857 (17)	C5—C6	1.3826 (12)
N12—C11	1.2812 (11)	C5—H5	0.9500
C1—C6	1.4033 (12)	C6—H6	0.9500
C1—C2	1.4091 (12)	C11—H11	0.9500
C1—C11	1.4584 (12)	C41—H41A	0.9800
C2—C3	1.3902 (12)	C41—H41B	0.9800
C3—C4	1.3928 (12)	C41—H41C	0.9800

C2—O2—H2	107.2 (11)	C6—C5—C4	120.40 (8)
N12—O13—H13	101.6 (11)	C6—C5—H5	119.8
C11—N12—O13	112.33 (7)	C4—C5—H5	119.8
C6—C1—C2	117.75 (8)	C5—C6—C1	121.44 (8)
C6—C1—C11	119.63 (8)	C5—C6—H6	119.3
C2—C1—C11	122.61 (8)	C1—C6—H6	119.3
O2—C2—C3	118.06 (8)	N12—C11—C1	120.08 (8)
O2—C2—C1	121.18 (8)	N12—C11—H11	120.0
C3—C2—C1	120.75 (8)	C1—C11—H11	120.0
C2—C3—C4	120.80 (8)	C4—C41—H41A	109.5
C2—C3—H3	119.6	C4—C41—H41B	109.5
C4—C3—H3	119.6	H41A—C41—H41B	109.5
C3—C4—C5	118.86 (8)	C4—C41—H41C	109.5
C3—C4—C41	120.51 (8)	H41A—C41—H41C	109.5
C5—C4—C41	120.60 (8)	H41B—C41—H41C	109.5

C6—C1—C2—O2	179.14 (7)	C3—C4—C5—C6	−0.06 (13)
C11—C1—C2—O2	−1.14 (14)	C41—C4—C5—C6	−178.02 (8)
C6—C1—C2—C3	0.13 (13)	C4—C5—C6—C1	0.24 (14)
C11—C1—C2—C3	179.86 (8)	C2—C1—C6—C5	−0.28 (13)
O2—C2—C3—C4	−178.99 (7)	C11—C1—C6—C5	179.99 (7)
C1—C2—C3—C4	0.04 (14)	O13—N12—C11—C1	179.95 (7)
C2—C3—C4—C5	−0.08 (13)	C6—C1—C11—N12	179.91 (8)
C2—C3—C4—C41	177.88 (7)	C2—C1—C11—N12	0.19 (14)

Hydrogen-bond geometry (Å, º)

Cg is the centroid of the C1–C6 ring.

D—H···*A*	*D*—H	H···*A*	*D*···*A*	*D*—H···*A*
O2—H2···N12	0.879 (18)	1.814 (18)	2.6066 (10)	149.0 (15)
O13—H13···O2^{i}	0.857 (17)	2.019 (17)	2.8132 (9)	153.7 (15)
O13—H13···O13^{ii}	0.857 (17)	2.611 (16)	2.8961 (14)	100.8 (12)
C3—H3···*Cg*^{iii}	0.95	2.71	3.4577 (9)	136
C11—H11···*Cg*^{iv}	0.95	2.73	3.4910 (9)	138

Symmetry codes: (i) −*x*+1, −*y*+1, −*z*+1; (ii) −*x*, −*y*+1, −*z*+1; (iii) −*x*+3/2, *y*+1/2, −*z*+1/2; (iv) −*x*+1/2, *y*−1/2, −*z*+1/2.

2,4-Dihydroxybenzaldehyde oxime (2)

Crystal data

$C_7H_7NO_3$	$F(000) = 320$
$M_r = 153.14$	$D_x = 1.516$ Mg m^{-3}
Monoclinic, $P2_1/c$	Mo $K\alpha$ radiation, $\lambda = 0.71075$ Å
$a = 3.7241$ (1) Å	Cell parameters from 13388 reflections
$b = 8.6902$ (2) Å	$\theta = 1.9$–32.1°
$c = 20.7570$ (5) Å	$\mu = 0.12$ mm^{-1}
$\beta = 92.501$ (2)°	$T = 100$ K
$V = 671.12$ (3) Å^3	Block, colourless
$Z = 4$	0.20 × 0.10 × 0.05 mm

Data collection

Rigaku FRE+ AFC12 with HyPix 6000 detector diffractometer	$T_{min} = 0.654$, $T_{max} = 1.000$
Radiation source: Rotating Anode, Rigaku FRE+	29482 measured reflections
Confocal mirrors, VHF Varimax monochromator	1537 independent reflections
Detector resolution: 10 pixels mm^{-1}	1482 reflections with $I > 2\sigma(I)$
profile data from ω–scans	$R_{int} = 0.039$
Absorption correction: multi-scan (CrysAlisPro ; Rigaku OD, 2017)	$\theta_{max} = 27.5°$, $\theta_{min} = 2.0°$
	$h = -4 \rightarrow 4$
	$k = -11 \rightarrow 11$
	$l = -26 \rightarrow 26$

Refinement

Refinement on F^2	Hydrogen site location: mixed
Least-squares matrix: full	H atoms treated by a mixture of independent and constrained refinement
$R[F^2 > 2\sigma(F^2)] = 0.040$	$w = 1/[\sigma^2(F_o^2) + (0.0229P)^2 + 1.3357P]$ where $P = (F_o^2 + 2F_c^2)/3$
$wR(F^2) = 0.092$	$(\Delta/\sigma)_{max} < 0.001$
$S = 0.86$	$\Delta\rho_{max} = 0.38$ e Å^{-3}
1537 reflections	$\Delta\rho_{min} = -0.21$ e Å^{-3}
113 parameters	
0 restraints	

Special details

Geometry. All esds (except the esd in the dihedral angle between two l.s. planes) are estimated using the full covariance matrix. The cell esds are taken into account individually in the estimation of esds in distances, angles and torsion angles; correlations between esds in cell parameters are only used when they are defined by crystal symmetry. An approximate (isotropic) treatment of cell esds is used for estimating esds involving l.s. planes.

Refinement. Refined as a 2-component twin.

Fractional atomic coordinates and isotropic or equivalent isotropic displacement parameters (Å^2)

	x	*y*	*z*	U_{iso}*/U_{eq}
O2	0.6604 (3)	0.13314 (13)	0.28983 (5)	0.0175 (3)
H2	0.568 (7)	0.056 (3)	0.3130 (12)	0.045 (7)*
O4	1.0469 (3)	0.64910 (12)	0.32704 (5)	0.0167 (3)
H4	1.132 (6)	0.639 (3)	0.2893 (11)	0.031 (6)*
O13	0.2536 (3)	−0.13686 (13)	0.41952 (6)	0.0213 (3)
H13	0.208 (7)	−0.200 (3)	0.3880 (12)	0.043 (7)*
N12	0.3984 (4)	−0.01346 (15)	0.38573 (6)	0.0161 (3)
C1	0.6052 (4)	0.24418 (16)	0.39524 (7)	0.0125 (3)
C2	0.7061 (4)	0.25485 (16)	0.33098 (7)	0.0129 (3)
C3	0.8530 (4)	0.38889 (17)	0.30720 (7)	0.0133 (3)
H3	0.9193	0.3946	0.2636	0.016*
C4	0.9020 (4)	0.51454 (17)	0.34786 (7)	0.0133 (3)
C5	0.8047 (4)	0.50773 (17)	0.41191 (7)	0.0148 (3)
H5	0.8379	0.5943	0.4395	0.018*
C6	0.6596 (4)	0.37332 (17)	0.43460 (7)	0.0141 (3)
H6	0.5947	0.3683	0.4783	0.017*
C11	0.4474 (4)	0.10553 (17)	0.42134 (7)	0.0144 (3)
H11	0.3805	0.1034	0.4650	0.017*

Atomic displacement parameters (Å^2)

	U^{11}	U^{22}	U^{33}	U^{12}	U^{13}	U^{23}
O2	0.0273 (6)	0.0106 (5)	0.0150 (5)	−0.0041 (5)	0.0047 (4)	−0.0036 (4)
O4	0.0249 (6)	0.0096 (5)	0.0161 (5)	−0.0052 (4)	0.0051 (4)	0.0002 (4)
O13	0.0335 (7)	0.0110 (5)	0.0194 (6)	−0.0095 (5)	0.0025 (5)	0.0019 (4)
N12	0.0189 (6)	0.0103 (6)	0.0191 (6)	−0.0029 (5)	0.0010 (5)	0.0030 (5)
C1	0.0127 (7)	0.0096 (6)	0.0151 (7)	0.0003 (5)	0.0005 (5)	0.0003 (5)
C2	0.0142 (7)	0.0101 (6)	0.0143 (7)	0.0008 (5)	−0.0003 (5)	−0.0023 (5)
C3	0.0149 (7)	0.0123 (7)	0.0126 (6)	0.0003 (6)	0.0020 (5)	0.0000 (5)
C4	0.0135 (7)	0.0087 (6)	0.0176 (7)	−0.0005 (5)	0.0009 (5)	0.0020 (5)
C5	0.0180 (7)	0.0106 (7)	0.0158 (7)	−0.0010 (6)	0.0015 (6)	−0.0027 (5)
C6	0.0158 (7)	0.0132 (7)	0.0135 (7)	−0.0005 (6)	0.0021 (5)	−0.0010 (5)
C11	0.0158 (7)	0.0117 (7)	0.0156 (7)	−0.0003 (6)	0.0003 (5)	0.0019 (5)

Geometric parameters (Å, º)

O2—C2	1.3655 (17)	C1—C11	1.456 (2)
O2—H2	0.91 (3)	C2—C3	1.387 (2)
O4—C4	1.3660 (17)	C3—C4	1.387 (2)
O4—H4	0.86 (2)	C3—H3	0.9500
O13—N12	1.4020 (16)	C4—C5	1.394 (2)
O13—H13	0.86 (3)	C5—C6	1.378 (2)
N12—C11	1.280 (2)	C5—H5	0.9500
C1—C6	1.398 (2)	C6—H6	0.9500
C1—C2	1.405 (2)	C11—H11	0.9500

C2—O2—H2	106.5 (16)	O4—C4—C3	121.64 (13)
C4—O4—H4	111.3 (15)	O4—C4—C5	117.43 (13)
N12—O13—H13	99.9 (16)	C3—C4—C5	120.93 (14)
C11—N12—O13	112.18 (13)	C6—C5—C4	118.93 (14)
C6—C1—C2	117.65 (13)	C6—C5—H5	120.5
C6—C1—C11	119.85 (13)	C4—C5—H5	120.5
C2—C1—C11	122.50 (13)	C5—C6—C1	121.98 (14)
O2—C2—C3	117.93 (13)	C5—C6—H6	119.0
O2—C2—C1	120.77 (13)	C1—C6—H6	119.0
C3—C2—C1	121.30 (13)	N12—C11—C1	120.25 (14)
C2—C3—C4	119.22 (13)	N12—C11—H11	119.9
C2—C3—H3	120.4	C1—C11—H11	119.9
C4—C3—H3	120.4		

C6—C1—C2—O2	−179.97 (14)	O4—C4—C5—C6	−179.63 (14)
C11—C1—C2—O2	−0.2 (2)	C3—C4—C5—C6	0.3 (2)
C6—C1—C2—C3	−0.3 (2)	C4—C5—C6—C1	−0.4 (2)
C11—C1—C2—C3	179.41 (14)	C2—C1—C6—C5	0.4 (2)
O2—C2—C3—C4	179.88 (13)	C11—C1—C6—C5	−179.33 (14)
C1—C2—C3—C4	0.2 (2)	O13—N12—C11—C1	178.31 (12)
C2—C3—C4—O4	179.71 (14)	C6—C1—C11—N12	−179.63 (14)
C2—C3—C4—C5	−0.2 (2)	C2—C1—C11—N12	0.6 (2)

Hydrogen-bond geometry (Å, º)

D—H···*A*	*D*—H	H···*A*	*D*···*A*	*D*—H···*A*
O2—H2···N12	0.91 (3)	1.77 (3)	2.5899 (17)	150 (2)
O4—H4···O2^{i}	0.86 (2)	1.85 (2)	2.7062 (16)	174 (2)
O13—H13···O4^{ii}	0.86 (3)	1.90 (3)	2.7583 (16)	171 (2)

Symmetry codes: (i) $-x+2, y+1/2, -z+1/2$; (ii) $x-1, y-1, z$.

2-Hydroxy-4-methoxybenzaldehyde oxime (3)

Crystal data

$C_8H_9NO_3$	$F(000) = 352$
$M_r = 167.16$	$D_x = 1.467$ Mg m^{-3}
Monoclinic, $P2_1/c$	Mo $K\alpha$ radiation, $\lambda = 0.71075$ Å
$a = 9.3591$ (13) Å	Cell parameters from 1379 reflections
$b = 6.2634$ (7) Å	$\theta = 3.3–30.2°$
$c = 13.6260$ (2) Å	$\mu = 0.11$ mm^{-1}
$\beta = 108.636$ (16)°	$T = 100$ K
$V = 756.87$ (15) Å^3	Plate, colourless
$Z = 4$	0.15 × 0.05 × 0.01 mm

Data collection

Rigaku FRE+ AFC12 with HyPix 6000 detector diffractometer
Radiation source: Rotating Anode, Rigaku FRE+
Confocal mirrors, VHF Varimax monochromator
Detector resolution: 10 pixels mm^{-1}
profile data from ω–scans
Absorption correction: multi-scan (CrysAlisPro; Rigaku OD, 2017)
$T_{\min} = 0.305$, $T_{\max} = 1.000$
5525 measured reflections
1686 independent reflections
1323 reflections with $I > 2\sigma(I)$
$R_{\text{int}} = 0.060$
$\theta_{\max} = 27.4°$, $\theta_{\min} = 2.3°$
$h = -11 \rightarrow 12$
$k = -7 \rightarrow 7$
$l = -17 \rightarrow 17$

Refinement

Refinement on F^2
Least-squares matrix: full
$R[F^2 > 2\sigma(F^2)] = 0.049$
$wR(F^2) = 0.158$
$S = 1.00$
1686 reflections
118 parameters
0 restraints
Hydrogen site location: mixed
H atoms treated by a mixture of independent and constrained refinement
$w = 1/[\sigma^2(F_o^2) + (0.1063P)^2]$ where $P = (F_o^2 + 2F_c^2)/3$
$(\Delta/\sigma)_{\max} < 0.001$
$\Delta\rho_{\max} = 0.26$ e Å^{-3}
$\Delta\rho_{\min} = -0.29$ e Å^{-3}

Special details

Geometry. All esds (except the esd in the dihedral angle between two l.s. planes) are estimated using the full covariance matrix. The cell esds are taken into account individually in the estimation of esds in distances, angles and torsion angles; correlations between esds in cell parameters are only used when they are defined by crystal symmetry. An approximate (isotropic) treatment of cell esds is used for estimating esds involving l.s. planes.

Fractional atomic coordinates and isotropic or equivalent isotropic displacement parameters (Å^2)

	x	y	z	U_{iso}*/U_{eq}
O2	0.63191 (14)	0.1847 (2)	0.42822 (9)	0.0193 (3)
H2	0.711 (3)	0.265 (5)	0.423 (2)	0.049 (7)*
O13	0.91351 (14)	0.6293 (2)	0.38674 (10)	0.0228 (4)
H13	0.981 (3)	0.524 (5)	0.388 (2)	0.062 (9)*
O41	0.10398 (13)	0.30632 (19)	0.36291 (8)	0.0182 (3)
N12	0.78766 (16)	0.5076 (2)	0.38782 (11)	0.0175 (4)
C1	0.52304 (18)	0.5260 (3)	0.36005 (11)	0.0145 (4)
C2	0.51014 (18)	0.3173 (3)	0.39480 (11)	0.0147 (4)
C3	0.37212 (18)	0.2374 (3)	0.39667 (12)	0.0158 (4)
H3	0.365066	0.097118	0.421199	0.019*
C4	0.24440 (19)	0.3667 (3)	0.36197 (12)	0.0150 (4)
C5	0.25337 (19)	0.5722 (3)	0.32479 (12)	0.0172 (4)
H5	0.165354	0.657670	0.299366	0.021*
C6	0.39104 (19)	0.6495 (3)	0.32543 (12)	0.0158 (4)
H6	0.397195	0.790761	0.301740	0.019*
C11	0.66646 (18)	0.6195 (3)	0.36181 (12)	0.0157 (4)
H11	0.670249	0.765245	0.343458	0.019*
C141	0.0866 (2)	0.0952 (3)	0.39792 (14)	0.0220 (4)
H14A	−0.018185	0.074061	0.395637	0.033*
H14B	0.153667	0.076825	0.469161	0.033*

H14C	0.112340	−0.009659	0.352899	0.033*

Atomic displacement parameters (Å^2)

	U^{11}	U^{22}	U^{33}	U^{12}	U^{13}	U^{23}
O2	0.0191 (7)	0.0148 (6)	0.0240 (7)	0.0044 (5)	0.0068 (5)	0.0056 (5)
O13	0.0187 (6)	0.0164 (7)	0.0360 (8)	−0.0006 (5)	0.0127 (5)	0.0018 (5)
O41	0.0181 (6)	0.0152 (7)	0.0220 (6)	0.0002 (5)	0.0075 (5)	0.0021 (4)
N12	0.0179 (7)	0.0163 (8)	0.0200 (7)	−0.0027 (5)	0.0083 (6)	−0.0003 (5)
C1	0.0200 (8)	0.0122 (8)	0.0122 (8)	−0.0001 (6)	0.0062 (6)	−0.0011 (6)
C2	0.0175 (8)	0.0147 (8)	0.0121 (7)	0.0024 (6)	0.0051 (6)	−0.0005 (6)
C3	0.0216 (9)	0.0118 (8)	0.0149 (8)	0.0013 (6)	0.0073 (6)	0.0007 (6)
C4	0.0180 (8)	0.0155 (9)	0.0119 (7)	−0.0001 (6)	0.0054 (6)	−0.0024 (6)
C5	0.0204 (8)	0.0150 (8)	0.0160 (8)	0.0045 (6)	0.0055 (6)	0.0006 (6)
C6	0.0235 (9)	0.0106 (8)	0.0139 (8)	0.0017 (6)	0.0068 (6)	0.0008 (6)
C11	0.0204 (9)	0.0131 (8)	0.0143 (8)	0.0004 (6)	0.0065 (6)	−0.0004 (5)
C141	0.0225 (9)	0.0144 (9)	0.0290 (9)	−0.0018 (7)	0.0082 (7)	0.0031 (7)

Geometric parameters (Å, º)

O2—C2	1.365 (2)	C3—C4	1.395 (2)
O2—H2	0.92 (3)	C3—H3	0.9500
O13—N12	1.4067 (18)	C4—C5	1.396 (2)
O13—H13	0.91 (3)	C5—C6	1.374 (2)
O41—C4	1.371 (2)	C5—H5	0.9500
O41—C141	1.432 (2)	C6—H6	0.9500
N12—C11	1.283 (2)	C11—H11	0.9500
C1—C2	1.409 (2)	C141—H14A	0.9800
C1—C6	1.405 (2)	C141—H14B	0.9800
C1—C11	1.458 (2)	C141—H14C	0.9800
C2—C3	1.393 (2)		

C2—O2—H2	104.4 (17)	C6—C5—C4	119.18 (15)
N12—O13—H13	100.6 (19)	C6—C5—H5	120.4
C4—O41—C141	117.95 (13)	C4—C5—H5	120.4
C11—N12—O13	111.75 (14)	C5—C6—C1	122.04 (15)
C2—C1—C6	117.58 (15)	C5—C6—H6	119.0
C2—C1—C11	123.02 (15)	C1—C6—H6	119.0
C6—C1—C11	119.37 (15)	N12—C11—C1	120.87 (16)
O2—C2—C3	117.11 (15)	N12—C11—H11	119.6
O2—C2—C1	121.63 (15)	C1—C11—H11	119.6
C3—C2—C1	121.26 (15)	O41—C141—H14A	109.5
C4—C3—C2	118.99 (15)	O41—C141—H14B	109.5
C4—C3—H3	120.5	H14A—C141—H14B	109.5
C2—C3—H3	120.5	O41—C141—H14C	109.5
O41—C4—C3	123.83 (15)	H14A—C141—H14C	109.5
O41—C4—C5	115.24 (14)	H14B—C141—H14C	109.5
C3—C4—C5	120.92 (16)		

C6—C1—C2—O2	178.92 (13)	C2—C3—C4—C5	0.7 (2)
C11—C1—C2—O2	−3.1 (2)	O41—C4—C5—C6	177.11 (13)
C6—C1—C2—C3	−1.2 (2)	C3—C4—C5—C6	−1.9 (2)
C11—C1—C2—C3	176.75 (14)	C4—C5—C6—C1	1.6 (2)
O2—C2—C3—C4	−179.21 (13)	C2—C1—C6—C5	−0.1 (2)
C1—C2—C3—C4	0.9 (2)	C11—C1—C6—C5	−178.10 (14)
C141—O41—C4—C3	−2.5 (2)	O13—N12—C11—C1	−178.61 (13)
C141—O41—C4—C5	178.56 (14)	C2—C1—C11—N12	5.8 (2)
C2—C3—C4—O41	−178.25 (14)	C6—C1—C11—N12	−176.33 (14)

Hydrogen-bond geometry (Å, º)

Cg is the centroid of the C1–C6 ring.

D—H···*A*	*D*—H	H···*A*	*D*···*A*	*D*—H···*A*
O2—H2···N12	0.92 (3)	1.81 (3)	2.6518 (19)	152 (2)
O13—H13···O41^{i}	0.91 (3)	1.89 (3)	2.7829 (18)	169 (3)
C141—H14*B*···O2^{ii}	0.98	2.62	3.412 (2)	138
C3—H3···O2^{ii}	0.95	2.70	3.570 (2)	154
C11—H11···*Cg*^{iii}	0.95	2.89	3.4524 (6)	128

Symmetry codes: (i) *x*+1, *y*, *z*; (ii) −*x*+1, −*y*, −*z*+1; (iii) −*x*+1, *y*+1/2, −*z*+1/2.